Orona-Návar, Carolina; Levchuk, Irina; Moreno-Andrés, Javier; Park, Yuri; Mikola, Anna; Mahlknecht, Jürgen; Sillanpää, Mika; Ornelas-Soto, Nancy

Removal of pharmaceutically active compounds (PhACs) and bacteria inactivation from urban wastewater effluents by UVA-LED photocatalysis with Gd^{3+} doped $BiVO_4$

Published in:
Journal of Environmental Chemical Engineering

DOI:
10.1016/j.jece.2020.104540

Published: 01/12/2020

Document Version
Peer-reviewed accepted author manuscript, also known as Final accepted manuscript or Post-print

Please cite the original version:
Orona-Návar, C., Levchuk, I., Moreno-Andrés, J., Park, Y., Mikola, A., Mahlknecht, J., Sillanpää, M., & Ornelas-Soto, N. (2020). Removal of pharmaceutically active compounds (PhACs) and bacteria inactivation from urban wastewater effluents by UVA-LED photocatalysis with Gd^{3+} doped $BiVO_4$. *Journal of Environmental Chemical Engineering*, *8*(6), Article 104540. https://doi.org/10.1016/j.jece.2020.104540

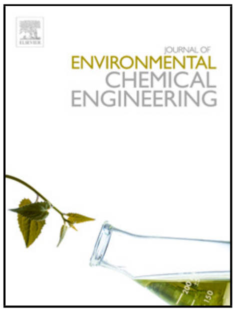

Removal of pharmaceutically active compounds (PhACs) and bacteria inactivation from urban wastewater effluents by UVA-LED photocatalysis with Gd^{3+} doped $BiVO_4$

Carolina Orona Návar (Conceptualization) (Methodology) (Investigation) (Validation) (Visualization) (Writing - original draft), Irina Levchuk (Conceptualization) (Methodology) (Investigation) (Validation) (Writing - original draft), Javier Moreno-Andrés (Conceptualization) (Methodology) (Investigation) (Validation) (Writing - original draft), Yuri Park (Supervision) (Writing - review and editing), Anna Mikola (Resources) (Supervision) (Writing - review and editing), Jürgen Mahlknecht (Supervision) (Writing - review and editing), Mika Sillanpää (Resources) (Supervision) (Writing - review and editing), Nancy Ornelas Soto (Resources) (Supervision) (Project administration) (Writing - review and editing) (Funding acquisition)

PII: S2213-3437(20)30889-7

DOI: https://doi.org/10.1016/j.jece.2020.104540

Reference: JECE 104540

To appear in: *Journal of Environmental Chemical Engineering*

Received Date: 6 August 2020

Revised Date: 16 September 2020

Accepted Date: 19 September 2020

Please cite this article as: Návar CO, Levchuk I, Moreno-Andrés J, Park Y, Mikola A, Mahlknecht J, Sillanpää M, Soto NO, Removal of pharmaceutically active compounds (PhACs) and bacteria inactivation from urban wastewater effluents by UVA-LED photocatalysis with Gd^{3+} doped $BiVO_4$, *Journal of Environmental Chemical Engineering* (2020), doi: https://doi.org/10.1016/j.jece.2020.104540

Removal of pharmaceutically active compounds (PhACs) and bacteria inactivation from urban wastewater effluents by UVA-LED photocatalysis with Gd^{3+} doped $BiVO_4$

Carolina Orona Návar [a], Irina Levchuk [b, c], Javier Moreno-Andrés [d], Yuri Park [e], Anna Mikola [c], Jürgen Mahlknecht [a], Mika Sillanpää [f, g, h, i, *], Nancy Ornelas Soto [a, *].

[a] Tecnologico de Monterrey, Escuela de Ingeniería y Ciencias, Ave. Eugenio Garza Sada 2501, Monterrey, N.L., México, 64849.

[b] Fine Particle and Aerosol Technology Laboratory, Department of Environmental and Biological Sciences, University of Eastern Finland, P.O. Box 1627, 70211 Kuopio, Finland

[c] Water and Wastewater Engineering Research Group, School of Engineering, Aalto University, PO Box 15200, FI-00076 Aalto, Finland.

[d] Department of Environmental Technologies, Faculty of Marine and Environmental Sciences, INMAR-Marine Research Institute, CEIMAR- International Campus of Excellence of the Sea, University of Cadiz, Spain.

[e] Department of Separation Science, LUT University, Sammonkatu 12, FI-50130 Mikkeli, Finland.

[f] Institute of Research and Development, Duy Tan University, Da Nang 550000, Vietnam.

[g] Faculty of Environment and Chemical Engineering, Duy Tan University, Da Nang 550000, Vietnam.

[h] School of Civil Engineering and Surveying, Faculty of Health, Engineering and Sciences, University of Southern Queensland, West Street, Toowoomba, 4350 QLD, Australia.

[i] Department of Chemical Engineering, School of Mining, Metallurgy and Chemical Engineering, University of Johannesburg, P. O. Box 17011, Doornfontein 2028, South Africa

* Corresponding authors. E-mail addresses: ornel@tec.mx (Nancy Ornelas Soto), mikaetapiosillanpaa@duytan.edu.vn (Mika Sillanpää)

Graphical Abstract

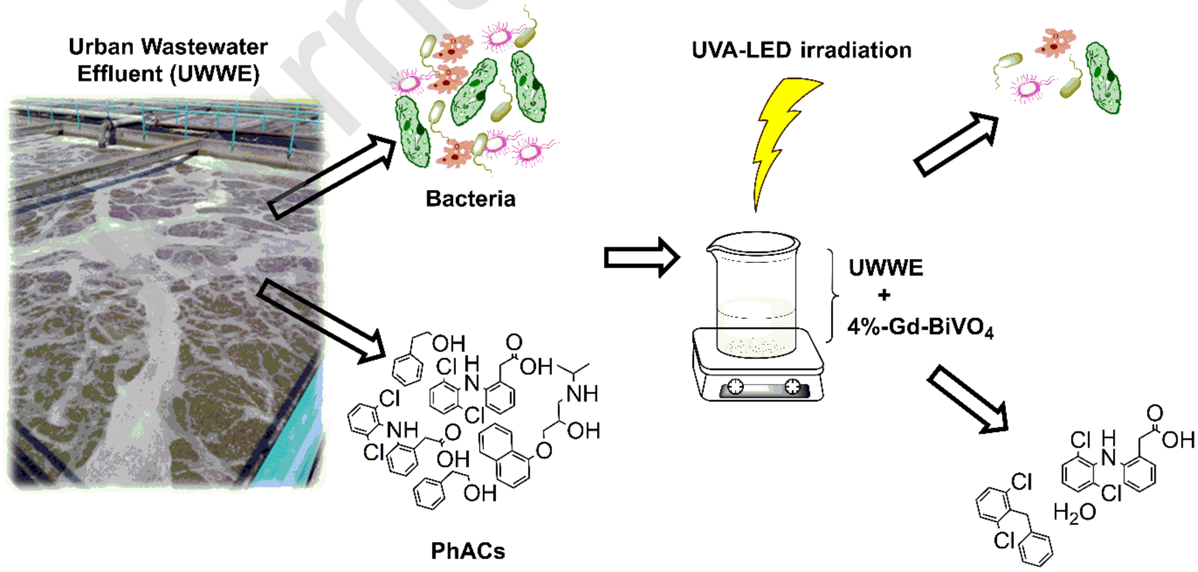

Highlights

- Gd^{3+} doped $BiVO_4$ photocatalyst was obtained by thermal method
- UVA-LED lamp was used as an eco-friendly light source in photocatalytic treatments
- 4 of the studied PhACs showed high photocatalytic removal from wastewater effluent
- Photocatalytic inactivation of bacteria present in wastewater effluent was studied
- *Enterococci* were the most sensitive bacteria to photocatalytic treatment

Abstract

In this study, gadolinium doped bismuth vanadate powders were synthesized, characterized, and tested as a potential photocatalyst for the removal of pharmaceutically active compounds (PhACs) and bacterial inactivation in a real wastewater effluent using UVA as irradiation source. X-ray diffraction (XRD) and X-ray photoelectron spectroscopy (XPS) studies revealed that the bismuth vanadate system was successfully doped with 4% of gadolinium in molar mass leading to the formation of a heterostructured photocatalyst.

Up to 98.3% of diclofenac was removed from pure water after 120 min through photocatalysis. However, the photocatalytic performance of the photocatalyst on wastewater effluent was rather variable due to the complexity of the matrix where 22 different PhACs were detected by means of Ultra Performance Liquid Chromatography-Triple Quadrupole Mass Spectrometry (UPLC-QqQ-MS/MS). High photocatalytic removal efficiency (80 – 100%) was observed for some of the studied PhACs (e.g. naproxen and furosemide) whereas moderate efficiency (40 – 70%) was observed for others (e.g. acetaminophen and azithromycin) after 180 min (UVA dose = 139.5 Wh m^{-2}, t_{30W} = 279 min^{-1}). Some of the studied PhACs like clarithromycin and Ibuprofen showed poor removal efficiency (< 30%). In disinfection tests, Total coliforms, *Escherichia coli, Enterococci*, and *Klebsiella pneumoniae* showed inactivation after direct UVA LED photolysis. Nevertheless, higher inactivation was achieved for *Enterococci* in the presence of the synthesized photocatalyst showing an increase of 41.1% in k_{max}.

Keywords: urban wastewater effluent, photocatalysis, Light-emitting diodes, pharmaceutically active compounds, photocatalytic disinfection, Gd-doped $BiVO_4$.

1. Introduction.

In the last few decades, the presence of pharmaceutically active compounds (PhACs) in the environment has gained attention due to the known negative effects that these chemical compounds may cause to ecosystems and human health. PhACs have been recurrently detected at low concentrations (ng L^{-1} - µg L^{-1}) in the effluents of wastewater treatment plants [1,2] as well as in recipient water bodies [3,4]. Potentially harmful contaminants such as macrolide antibiotics (e.g. erythromycin, clarithromycin, azithromycin), 17-alpha-ethinylestradiol, amoxicillin, and ciprofloxacin among others, are included in the surface water Watch List Directive 2018/840/EU to be carefully monitored by member states of the European Union [5]. The conventional wastewater treatment processes (e.g. activated sludge, filtration, and disinfection) are not efficient enough in PhACs removal [1,6]. Therefore, effluent discharges from wastewater treatment plants (WWTP) have been identified as important anthropogenic sources of PhACs [7,8]. In addition to effective PhACs removal, the efficient elimination of pathogens from water is very important in order to prevent the transmission of diseases by contaminated water. UV light, chlorination, and ozonation have been widely used as effective methods for water disinfection, however, the formation of toxic by-products is a major drawback [9].

The development and implementation of advanced treatment processes have arisen to complement the conventional treatment methods to achieve greater efficiency in the disinfection and elimination of PhACs from urban wastewater effluents. Advanced oxidation processes (AOPs) have proven to be an effective approach to this problem. Specifically, heterogeneous photocatalysis through the generation of reactive oxygen species (e.g. •OH, $•O_2^-$) achieves the degradation of PhACs [6,7,10]. The inactivation of bacteria using photocatalytic processes has also been widely demonstrated [9,11].

Different photocatalysts have been used for those purposes, among them, TiO_2 has been considered an excellent photocatalyst because it has desirable characteristics such as chemical stability, and low costs [12]. However, the wide band gap of TiO_2 (3.2 eV) limits its photocatalytic response to the UV region of the light spectrum, which represents about 3 to 5% of the solar spectrum [13]. Therefore, the need has arisen to study photocatalysts that, besides being effective under UV light ($100 < \lambda < 400$ nm) , show good photocatalytic activity under visible light ($\lambda > 400$ nm) [13]. Such photocatalysts will lead to the implementation of more sustainable technologies that take advantage of most of the solar spectrum for both disinfection and removal of PhACs from water [14,15]. To overcome drawbacks of solar technologies, such as limitation of daylight hours, large areas needed and high installation costs, the use of different types of lamps has been widely investigated and currently they are the most common light source used in photocatalytic processes instead of using direct solar irradiation [16,17]. Special attention has been directed to light-emitting diodes (LED) lamps since, from the green chemistry point of view, the use of conventional UV light sources constitutes an environmental problem arising at the step of the utilization of lamps containing hazardous mercury. Light-emitting diodes (LED) could be an eco-friendly alternative for traditional UV irradiation sources since they do not contain toxic elements such as mercury. It should be noted that in comparison with conventional UV lamps, high power LED are more expensive but show longer life time (up to 100,000 h) and better resistance to mechanical impact, also they are more energy efficient and have a compact size [16,18].

Among photocatalysts, bismuth vanadate ($BiVO_4$) has shown excellent visible and UVA (315 – 400 nm) adsorption [19,20]. This wide-range absorption makes it a photocatalyst with potential for use both in disinfection, taking advantage of UV absorption, as well as in the photocatalytic degradation of PhACs, taking advantage of the UV-Vis adsorption range, whether the radiation comes from a lamp o directly from the sun [15,21–23]. Moreover, it has been proved that $BiVO_4$ can significantly enhance its photocatalytic activity through rare-earths doping for both removal of organic pollutants and bacteria inactivation [24–26]. For instance, drastically greater photocatalytic performance of Er^{3+} and Y^{3+} doped $BiVO_4$ compared to pristine $BiVO_4$ for *Escherichia coli* inactivation and methanol oxidation in deionized water under UV-Vis irradiation have been reported [27]. Gadolinium (Gd^{3+}) has demonstrated superior results in improving the activity of various photocatalysts (e.g. SnO_2, TiO_2, and Bi_2O_3) [25,28,29]. This may be due to its electronic structure with a partially occupied “d” and “f” orbitals that facilitates the formation of complexes promoting the adsorption of the contaminants on the surface of the photocatalyst [30]. Despite the superior photocatalytic efficiencies reported for the rare earth doped $BiVO_4$ compared to un-doped $BiVO_4$, their performance in real wastewater effluent for PhACs removal and bacteria inactivation has been scarcely studied [31]. In addition, recent studies highlight the critical importance of assessment of heterogeneous photocatalysis under realistic water matrices, which could avoid misleading conclusions of its applicability [32,33].

Herein, the photocatalytic efficiency of Gd^{3+} doped $BiVO_4$ was evaluated through the degradation of 22 different PhACs detected in real urban wastewater effluent. The effect of the photocatalyst load was also investigated. Moreover, photocatalytic inactivation of Total coliforms, *Escherichia coli, Enterococci*, and *Klebsiella pneumoniae* that were naturally present in the wastewater effluent was assessed using a UVA-LED lamp as irradiation source.

2. Materials and Methods.

2.1 Chemicals

All chemicals used were analytical grade reagents. Bismuth (III) nitrate pentahydrate ($Bi(NO_3)_3 \cdot 5H_2O$), ammonium metavanadate (NH_4VO_3), Gadolinium (III) chloride hexahydrate ($GdCl_3 \cdot 6H_2O$), ethylene glycol, α-d-Glucose, and diclofenac were purchased from Sigma-Aldrich and were used without further purification. HPLC grade solvents were used for chromatographic analysis. The HPLC grade methanol was purchased from Scharlau (Spain).

The cartridges for solid phase extraction (Oasis HLB 200 mg) were received from Waters Chromatography Europe BV. Analytical standards of measured pharmaceuticals were received from suppliers listed elsewhere [34].

2.2 Preparation of Gd^{3+} doped $BiVO_4$

Gd^{3+} doped Bismuth vanadate ($BiVO_4$) was prepared following a modified methodology of the thermal synthesis proposed by Yin et al. 2009 [35]. Briefly, 3 mmol of $Bi(NO_3)_3{\cdot}5H_2O$ and 3 mmol of NH_4VO_3 were dissolved in 30 mL of ethylene glycol at 60°C controlled in an oil bath. Once a clarifying solution was formed a certain amount of $GdCl_3{\cdot}6H_2O$ was added to obtain 4% of Gadolinium in molar mass. This was the optimal Gd^{3+} content according to our previous study about Gd^{3+} doped $BiVO_4$ in which photocatalysts using different dopant concentrations were tested through the degradation of bisphenol A in water. Those results are available as supplementary information (Figure S3). After the solution was vigorously stirred for 30 minutes, 400 mg of as-prepared carbonaceous template spheres were dispersed to promote the interaction of the dopant with the metal ions while they precipitated on the surface of the templates [35]. The solution was kept in the oven at 60°C for 12 hours, then the temperature was raised to 100°C and kept for another 12 hours. Afterward, the precipitate was collected, washed several times with distilled water and ethanol, and dried at 80°C overnight. The dried powder was calcined for 2 hours at 550°C using a ramp of 10°C min^{-1}. The prepared photocatalysts were denoted as 4%-Gd-$BiVO_4$.

Carbonaceous template spheres were prepared by hydrothermal method as follows: 0.5 mol of α-D-Glucose was dissolved in 80 mL of pure water. The solution was placed in a 100 mL autoclave and heated at 180°C for 4.5 hours. After cooling down at room temperature, the precipitates were collected and washed with water and ethanol several times. Finally, the product was dried at 80°C for 12 hours [36].

2.3 Characterization techniques

An X-ray powder diffractometer (PANalytical Empyrean) with Co Kα radiation source (λ=1.7809 Å) at 40 kV and 30 mA was used to obtain X-ray diffraction (XRD) patterns and crystallographic information. The morphology and particle size of the as-prepared photocatalysts were observed using a scanning electron microscope (SEM, Hitachi S-4800). The N_2 sorption experiments were carried out in a TriStar II Plus and specific surface area was estimated using the Brunauer-Emmett-Teller (BET) method. The UV-Vis diffuse reflectance spectra (DRS) were determined using a UV-Vis spectrometer (Agilent Cary 5000) in the wavelength range of 250 to 800 nm using spectralon standard as reference. The surface composition and electronic states of elements present in the photocatalyst were obtained by X-ray photoelectron spectroscopy (XPS) performed on an ESCALAB 250Xi (Thermo Fisher

Scientific) spectrophotometer with monochromatic Al-Kα (1486.6 eV) X-ray source. Raman spectra were acquired with a Renishaw inVia Micro Raman spectrometer. Sample excitation was carried out with a 514 nm green laser. The presence of dissolved metals and rare earth (Bi, V, and Gd) was evaluated by analyzing the wastewater samples after photocatalytic tests using inductively coupled plasma optical emission spectroscopy (ICP-OES) on an Agilent 5110.

2.4 Photocatalytic experiments

2.4.1. Photocatalytic decomposition of diclofenac in ultra-pure water

In order to study the effect of 4%-Gd-$BiVO_4$ concentration on the rate of photocatalytic reaction, the experiments were conducted in ultra-pure water using diclofenac (DCF, initial concentration 10 mg L^{-1}) as a model contaminant. Nonsteroidal anti-inflammatory drug diclofenac was chosen as a model pollutant because it is widely used and frequently found in urban wastewater effluents [37]. All photocatalytic tests with DCF were performed in batch mode under constant stirring at ambient temperature (20 ± 2°C) using PYREX glass Erlenmeyer flask (total volume 150 mL). Different concentrations of photocatalyst (from 0.25 to 2 g L^{-1}) were tested. Each experiment was repeated at least twice. Two identical flasks wrapped with aluminum foil (except the bottom of the flasks) were located on the top of the UVA-LED lamp (λ=370 nm, length 30 cm and widths 8 cm). The UVA LED intensity (46.5 ± 0.6 W m^{-2}) was measured on the reactor surface using UV AB Light Meter (General UV513AB). The accumulated UVA dose (using LED) was calculated to facilitate the comparison of PhACs degradation kinetics when different experimental conditions are used in other studies. It is widely assumed that applied UV dose is obtained by multiplying the intensity by the time [6].

The volume of model DCF solution used in experiments was 100 mL. To ensure the adsorption-desorption equilibrium between photocatalyst and DCF, the model solution was stirred for 30 min in the dark. After that, the UVA-LED was turned on and samples were taken at desired time intervals. After sampling, filtration with regenerated cellulose syringe filters (0.22 μm) was performed in order to remove photocatalyst. Filtered samples were further analyzed by means of High Performance Liquid Chromatography (HPLC, UFLC Shimadzu) equipped with a UV-Vis detector (SPD-20AV) at a wavelength of 275 nm using a C-18 column (Kinetex, 5μm, 150 x 4.6 mm). Methanol and water (0.1% formic acid) were used as a mobile phase in a volume ratio of 75:25. The isocratic mode was used with a flow rate of 1 mL min^{-1}. Adsorption (in absence of UVA LED) and photolysis (in absence of photocatalyst) experiments were conducted with DCF model solution as reference tests.

2.4.2. Photocatalytic degradation of PhACs in urban wastewater effluent

Photocatalytic experiments using wastewater effluent as a reaction medium were conducted in a volume of 110 mL. The optimal concentration of 4%-Gd-$BiVO_4$ photocatalyst for experiments with urban wastewater effluent was selected based on tests conducted with diclofenac in ultra-pure water (model solution). Real urban wastewater effluent was used for the following studies on photocatalytic decomposition of PhACs present in urban wastewater effluent and disinfection studies. The wastewater effluent was taken from the Viikinmäki Wastewater Treatment Plant (WWTP) located in Helsinki (Finland). This WWTP processes wastewater from Industry and households (85% of total influent) applying a method based on chemically enhanced pre-sedimentation and enhanced nitrogen removal in activated sludge and post-denitrifying filters. Samples were collected in amber glass flasks, preserved in the fridge at 4 °C, and used within the next day. The main physicochemical characteristics (Table 1) of used wastewater effluent were measured using standard methods [38]. Total Organic Carbon (TOC) measurements were performed in non-purgeable carbon (NPOC) mode by means of Shimadzu TOC-L analyzer.

Table 1. Physicochemical characterization of urban wastewater effluent.

Parameter	**Concentration in effluent (unit)**
BOD_7	8.6 (mg L^{-1})
COD	57 (mg L^{-1})
TOC	22.2 (mg L^{-1})
Suspended Solids (SS)	6.2 (mg L^{-1})
Total P	0.07 (mg L^{-1})
Total N	6.3 (mg L^{-1})
NH_4-N	1.7 (mg L^{-1})
NO_3-N	2.0 (mg L^{-1})
Alkalinity	2.3 (mmol L^{-1})
SO_4^{2-}	100.6 (mg L^{-1})
Cl^-	80.6 (mg L^{-1})
Total iron	0.5 (mg L^{-1})
pH	7.2
Conductivity	70.1 (mS m^{-1})

Transmittance	79.2% (370 nm)

The concentration of PhACs in wastewater effluent was analysed before and after photocatalytic tests as well as after reaching adsorption equilibrium (30 min in dark before switching on the UVA LED lamp). Measurements were also performed after reference tests such as photolysis (180 min) and adsorption (210 min). Analysis of PhACs was performed as reported earlier [34]. Briefly, Solid Phase Extraction (SPE) was applied as a pretreatment method using HLB cartridges (Oasis, 200 mg). Conditioning of HLB cartridges was conducted with 8 mL of methanol and 8 mL of Milli-Q water. Consequently, samples (100 mL) were passed through cartridges. Finally, cartridges were washed with Milli-Q water (10 mL) and dried in air. Elution was performed using 10 mL of methanol. Extracts were evaporated under a nitrogen stream and reconstructed in a mixture of water and methanol (75:25). Qualification and quantification of PhACs were conducted using Bruker EVOQ Elite (Bruker, Billerica, MA) Ultra Performance Liquid Chromatography – Triple Quadrupole Mass Spectrometry (UPLC-QqQ-MS/MS) with C-18 column (100 x 2.1 mm; particle size 2 µm) and electrospray interface. The injection volume was 10 µL and the flow rate was 0.4 mL/min in positive and negative ionization modes. The aqueous mobile phases used for measurements conducted in positive ionization mode were a mixture of 10 mmol formic acid and ammonium formate (pH 3.2), while 100% methanol was used as organic mobile phase. Aqueous mobile phases applied for analysis performed in negative ionization mode were 5 mmol ammonium acetate/ammonia (pH 8), while organic mobile phase consisted of 100% methanol. Multiple reaction monitoring (MRM) was used for data acquisition. Obtained data were processed with Bruker MS Workstation 8.1 Software.

2.4.3. Photocatalytic disinfection tests

Wild microorganisms naturally present in wastewater were selected as target bacteria. Thus, quantification of Total coliforms, *Escherichia coli (E. coli)*, and *Enterococci* were carried out by standard plating on commercial media: Chromogenic Collinstant Agar (Scharlab) and Slanetz & Bartley Agar (Panreac). Likewise, TCBS Thiosulfate Citrate Bile Salts Sucrose Agar (Pronadisa, Condalab) was used as solid media for *Klebsiella pneumoniae* (99.6%) which was identified by the amplification and sequencing of a fragment of 16S rDNA, as explained in previous studies [39]. The plates were incubated at 30 ± 2 °C for 24 - 48 h according to the specific bacteria.

For UVA-LED based photocatalytic disinfection experiments an optimal concentration of 4%-Gd-$BiVO_4$ (1 gL^{-1}) was chosen based on experiments of DCF decomposition (Section 2.4.1). The volume of wastewater was 75 mL. The solution was kept in the dark for 30 min to reach adsorption-desorption equilibrium and after that, the UVA-LED lamp was turned on. Samples were withdrawn at set time intervals and the total duration of disinfection experiments was 1 h.

The analysis of surviving organisms was enumerated by the spread-plate method. At longer exposure times, larger volumes of wastewater were plated by the membrane filtration method (gridded membranes of 0.45 μm). Colony-Forming Units (CFU) concentrations from samples measured by spread-plate as well as membrane filtration techniques were in good agreement. Results were expressed as the mean microbiological concentration of each sample (three replicates), in CFU mL^{-1}. The disinfection efficiency was determined according to time–response curves where the logarithmic reduction of the survival of microorganisms is represented. In order to quantify the disinfection performance, kinetic modeling was applied to experimental data. Log-linear approach ($\mathrm{Log}(N/N_0) = -\mathrm{k} \cdot \mathrm{t}$), was suitable ($R^2 \geq 0.78$ in all cases) for describing microbial inactivation curves.

3. Results and discussion.

3.1 Characterization of 4%-Gd-BiVO$_4$

The crystalline structure of the synthesized 4%-Gd-BiVO$_4$ was determined by XRD analysis. The diffraction patterns (Figure 1) showed a good fitting with the Tetragonal dreyerite BiVO$_4$ structure (JCPDS file 00-014-0133). Additionally, Rietveld refinement revealed the slight presence of two additional crystalline structures: monoclinic Bi$_{0.95}$Gd$_{0.05}$VO$_4$ (JCPDS file 00-033-0123) and Tetragonal Bi$_2$O$_3$ phase (JCPDS file 01-078-1793). The detailed XRD profile data obtained by Rietveld refinement for bare BiVO$_4$ and 4%-Gd-BiVO$_4$ have been included as supplementary information (Figures S1 and S2). The presence of the three crystalline phases may induce the formation of heterostructures that promotes an efficient electron-hole pairs separation and an effective diffusion of these charge carriers towards photocatalyst´s surface, improving its photocatalytic activity [40,41]. From XRD analysis it can also be inferred that the presence of Gd^{3+} ions influences the formation of the crystalline structure. Lattice parameters, unit cell volume, and the goodness of chi-square (χ^2) fitting parameter were calculated and are shown in Table 2.

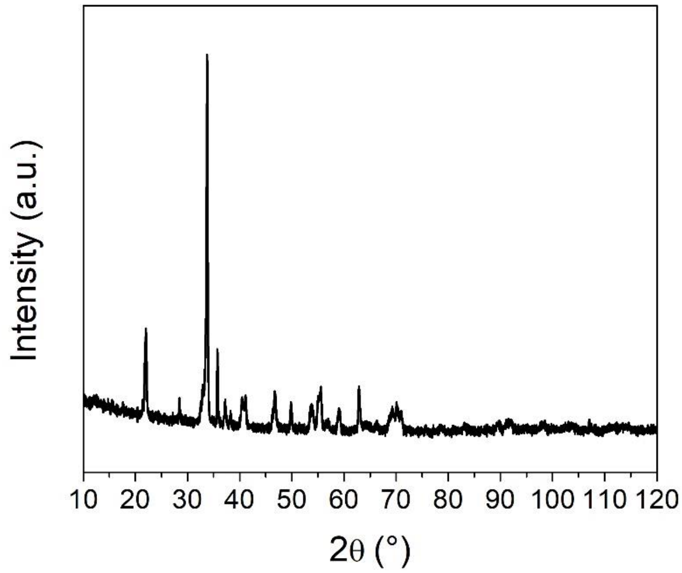

Figure 1. XRD pattern of the prepared 4%-Gd-$BiVO_4$

Table 2. Crystallographic parameters of 4%-Gd-$BiVO_4$

Material	Phases	Spatial group	Lattice Parameters			Unit cell volume (Å^3)	Chi-square (χ^2)	Crystallite size (nm)
			a (Å)	B (Å)	C (Å)			
4%-Gd-$BiVO_4$	*t-$BiVO_4$	I41/amd	7.34745	7.34745	6.44067	347.700	1.203	89
	$Bi_{0.95}Gd_{0.05}VO_4$	P21/c	5.15209	5.15210	11.74611	311.789		
	*t-Bi_2O_3	P-421c	7.68477	7.68477	5.61992	331.889		

* t = tetragonal

Figure 2 shows the SEM micrograph of the as prepared photocatalyst obtained by a thermal method. Sphere and peanut-like nanoparticles randomly aggregated can be identified. It is observed that the nanoparticles were sintered during the calcination step. This particular morphology has been previously reported for pristine $BiVO_4$ [35,42], and most studies agree that the obtained morphology of $BiVO_4$ depends on the method and conditions used during the synthesis [15,43]. The average size of the nanoparticles is 89 nm, which is in agreement with the crystallite size obtained by XRD analysis.

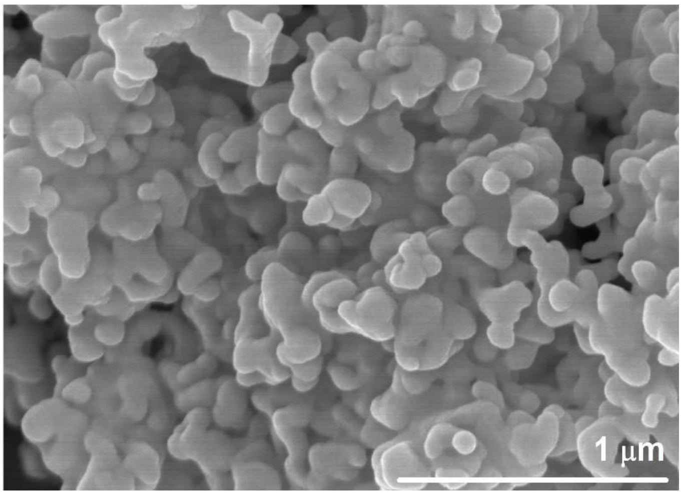

Figure 2. SEM image of the synthesized 4%-Gd-$BiVO_4$ photocatalyst

The surface area of pristine t-$BiVO_4$ has been previously reported to be in the range of 1.24 to 5 m^2 g^{-1} [19]. It is known that this material generally presents a low surface area. The measured value of the BET surface area of 4%-Gd-$BiVO_4$ was 5.64 m^2 g^{-1}. Compared to pristine t-BiVO4, the surface area of the photocatalyst surface area was not significantly increased or decreased after incorporation of Gd^{3+} ions. Therefore, the surface area may not have a significant effect on the photocatalyst performance.

The chemical species present on the synthesized photocatalyst were analyzed by means of X-ray photoelectron spectroscopy (XPS). The survey spectra are shown in Figure 3a where all the expected elements (Bi, V, O, and Gd) can be identified. The incorporation of Gd^{3+} ions on the $BiVO_4$ crystalline structure was confirmed through the obtained high resolution XPS spectra of Gd 4d showing a peak at 142 eV (Figure 3e), as well as the presence of a Gd 4f and Gd 3d peaks at the survey spectra. Gadolinium probably incorporates by substitution on Bi^{3+} sites because of the smaller ionic size of Gd^{3+} (0.0938 nm) compared with Bi^{3+} (0.103 nm). The high-resolution XPS spectra of O 1s are shown in Figure 3b where the peak at 529.8 eV of binding energy can be related to the presence of O_2^- anions. Similarly, Figure 3c indicates the presence of V^{5+} according to the identified peaks at 516 and 524 eV that correspond to V $2p_{1/2}$ and V $2p_{3/2}$ orbitals respectively [44]. In Figure 3 d two symmetric peaks are shown for Bi $4f_{5/2}$ and Bi $4f_{7/2}$ at binding energies around 164 and 159 eV respectively, which are designated to Bi^{3+} chemical state [45].

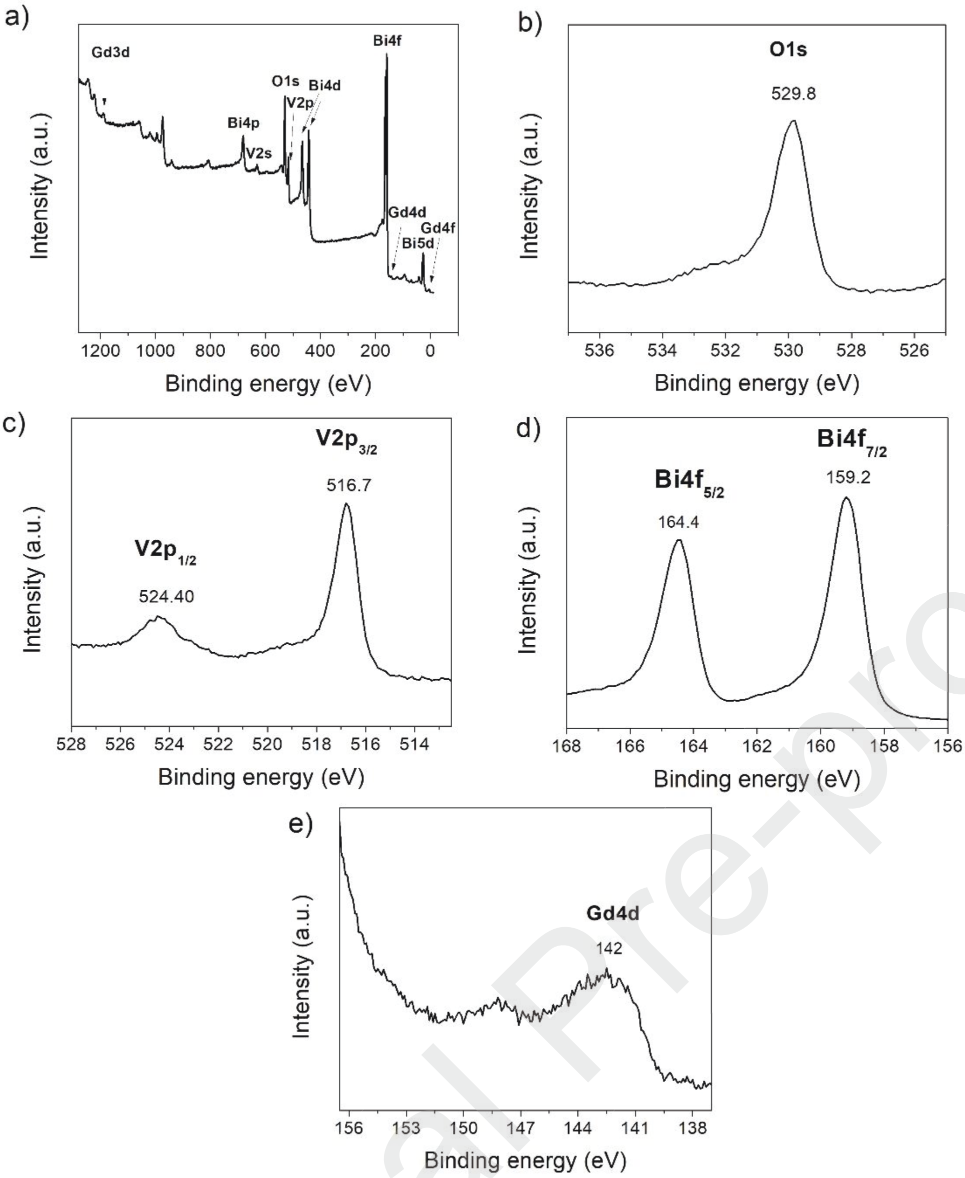

Figure 3. XPS spectra of 4%- Gd-BiVO$_4$ photocatalyst: (a) survey, (b) O 1s peak, (c) V 2p peaks, (d) Bi 4f peaks, and (e) Gd 4d peak

According to diffuse reflectance UV-vis spectra shown in Figure 4, 4%-Gd-BiVO$_4$ exhibited strong absorption in the UV-visible region. Band gap energy of the synthesized material was determined through Kubelka-Munk function (KMF), which can be expressed as shown in equation 1.

$$\mathrm{KMF} = \mathrm{F}(\mathrm{R}_\infty) = (1 - \mathrm{R}_\infty)^2/2\mathrm{R}_\infty = \mathrm{k/s} \qquad \text{Eq. (1)}$$

Where R is the absolute reflectance of a layer with an infinite thickness, K is the absorption coefficient, and S is the scattering coefficient. KMF values were multiplied by photon energy to the power of 0.5 and plotted vs energy of the incident light. The extrapolation of the linear region (Figure 4, inset) provided a band gap of 2.46 eV for 4%-Gd-$BiVO_4$.

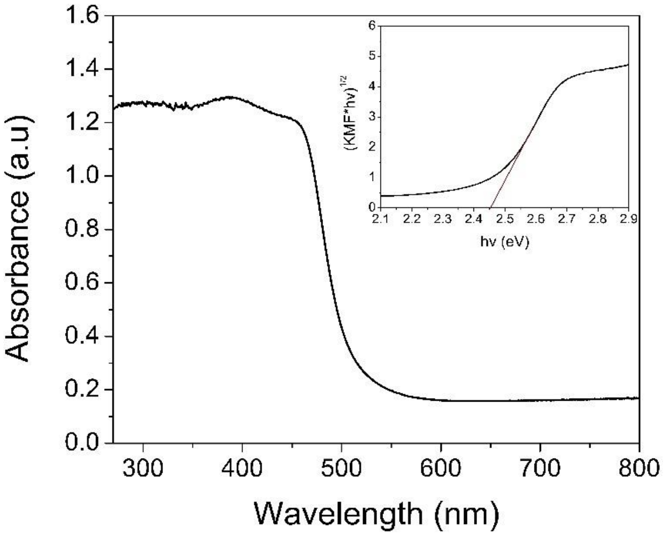

Figure 4. Diffuse reflectance UV-Vis spectra and Kubelka-Munk plot of 4%-Gd-$BiVO_4$.

3.2 Photocatalytic efficiency of 4%-Gd-$BiVO_4$

3.2.1 Effect of 4%-Gd-$BiVO_4$ concentration on diclofenac degradation

The effect of photocatalyst concentration on the rate of photocatalytic reaction was studied. Figure 5a shows DCF decomposition (as model compound) as a function of contact time with different 4%-Gd-$BiVO_4$ loadings. It is observed that the dependence of DCF concentration on the contact time follows a linear behavior in the studied time interval, indicating zero-order kinetics. The calculated initial disappearance rates for DCF degradation at different 4%-Gd-$BiVO_4$ loadings are shown in Figure 5b. As can be observed from Figure 5b, the photocatalyst load increases and so does the DCF initial disappearance rate. The most significant increment was observed from 0.25 g L^{-1} to 0.5 g L^{-1} where the initial disappearance rate was doubled from 0.256 to 0.511 μmol L^{-1} min^{-1}. Further increase of photocatalyst loading did not affect significantly the initial DCF degradation rate. It is important to notice that these tests have been done in a pure water DCF solution, however, loads as high as 2 g L^{-1} in a real effluent could cause such turbidity that it would significantly reduce light transmission, in addition to increasing the cost. Hence, 1 g L^{-1} was considered as an adequate 4%-Gd-$BiVO_4$ dose to ensure the effective absorption of photons. Also, other aspects were considered for choosing the optimal photocatalyst load, for instance, the fact that several authors have used the same photocatalyst load (1 g L^{-1}) for studying organic contaminants removal from water. This makes easier the comparison between different studies [15,43]. Moreover, it is desirable that the synthesized photocatalyst (4%-Gd-$BiVO_4$), in addition to removing PhACs, efficiently inactivate bacteria. Hence, studies in photocatalytic disinfection were consulted as well and considered as reference for choosing the optimal photocatalyst load. Thus, Booshehri et al., (2017) obtained the best inactivation kinetics for *E. coli*, *E. faecalis* and *F. solani* in distilled water (10 L reactor) using 1 g L^{-1} of Ag/$BiVO_4$ under solar light. It is important to note that this parameter strongly depends on the type of bacteria and other experimental conditions. Finally, in accordance with the obtained results from tested conditions as well as revised literature, 1 g L^{-1} of 4%-Gd-$BiVO_4$ was chosen as an optimal dose for both photocatalytic and disinfection experiments.

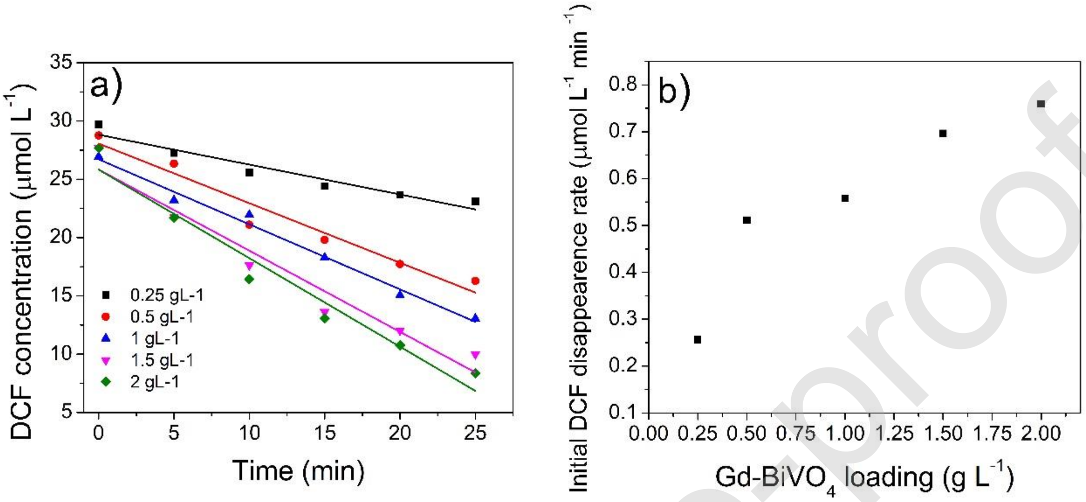

Figure 5. a) Results of DCF degradation with different loadings of 4%-Gd-$BiVO_4$. b) Influence of 4%-Gd-$BiVO_4$ loading on initial disappearance rate of DCF degradation

Figure 6 depicts the photocatalytic decomposition of DCF in model solution. Adsorption and photolysis effect can be neglected since no significant changes were observed on DCF concentration after 180 min (UVA dose = 139.5 Wh m^{-2}, t_{30W} = 279 min^{-1}). In the presence of 4%-Gd-$BiVO_4$ and under UVA-LED irradiation, DCF concentration considerably decreased up to 50% in the first 20 minutes, then a slower decrease was observed until DCF disappeared almost completely (98.3%) after 120 min (UV dose: 93 Wh m^{-2}, t_{30W} = 186 min^{-1}) using 1 g L^{-1} of photocatalyst. Other studies are reporting similar behavior of DCF in water [46]. For instance, Tbessi et al., (2019) achieved ~90% of DCF degradation (initial concentration of 10 mg L^{-1}) in distilled water within the first 120 min using Mn-Ag-TiO_2. Similarly, Sarasidis et al., (2014) reached 99.5% of DCF (initial concentration of 2.5 mg L^{-1}) degradation in spiked groundwater after 120 min using TiO_2. Both studies used a UVA lamp as radiation source.

Although the studies carried out in the diclofenac model solution gave us an idea of the efficiency of 4%-Gd-$BiVO_4$ in the degradation of organic pollutants, it cannot be assumed that the photocatalyst will behave in the same way when used in a more complex matrix. Therefore, it is important to carry out the photocatalytic study in real water matrices to have reliable evidence of photocatalysts applicability [49].

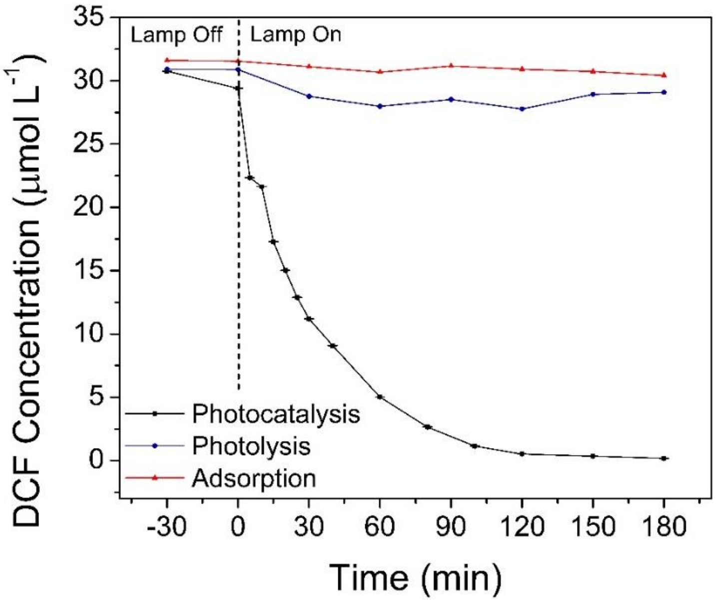

Figure 6. Photocatalytic degradation of DCF in ultra-pure water under UVA-LED irradiation (UVA dose = 139.5 Wh m^{-2}, t_{30W} = 279 min^{-1}) using 1 g L^{-1} of 4%-Gd-$BiVO_4$.

3.2.2 Photocatalytic treatment in wastewater effluent for PhACs removal

It is of high importance to study the efficiency of novel photocatalytic materials not only using model solutions but also real wastewater [50]. Hence, photocatalytic tests were also performed using real urban wastewater effluent. Concentrations of 22 PhACs such as anti-inflammatory compounds (acetaminophen, salicylic acid, ibuprofen, naproxen, diclofenac, and ketoprofen), lipid regulator (gemfibrozil), diuretics (furosemide, hydrochlorothiazide), macrolides (azithromycin, clarithromycin), sulfonamides (sulfadiazine, sulfamethoxazole), quinolones (ofloxacin, norfloxacin, ciprofloxacin), dihydrofolate (trimethoprim), beta-blockers (propranolol, atenolol), psychiatric drugs (carbamazepine, caffeine) and medicine for asthma treatment (albuterol) were measured in wastewater effluent before photocatalytic tests and results are shown in Table 3.

Table 3. A raw concentration of pharmaceutically active compounds presents in urban wastewater effluent before photocatalytic treatment.

Type	Contaminant	Concentration in effluent (ng L^{-1})	LOD[1] (ng L^{-1})	LOQ[2] (ng L^{-1})
Anti-inflammatories	Acetaminophen	144.3 ± 29.9	0.5	1.8
	Salicylic Acid	60.6 ± 25.7	1.3	4.4
	Ibuprofen	13466.4 ± 1278.2	1	3.5

	Naproxen	2817.6 ± 75.8	0.3	0.9
	Diclofenac	2062.1 ± 201.7	0.1	0.2
	Ketoprofen	359.5 ± 21.2	0.1	0.3
Lipid Regulators	Gemfibrozil	51.0 ± 4.0	<0.1	<0.1
Diuretics	Furosemide	2291.4 ± 29.8	<0.1	<0.1
	Hydrochlorothiazide	629.9 ± 12.0	<0.1	<0.1
Macrolides	Azithromycin	892.0 ± 186.8	<0.1	<0.1
	Clarithromycin	196.4 ± 27.0	<0.1	<0.1
Sulfonamides	Sulfadiazine	33.5 ± 1.7	<0.1	<0.1
	Sulfamethoxazole	84.9 ± 2.4	<0.1	<0.1
Quinolones	Ofloxacin	967.8 ± 120.6	<0.1	<0.1
	Norfloxacin	76.1 ± 8.8	<0.1	0.1
	Ciprofloxacin	9687.2 ± 1147.6	0.1	0.2
Dihydrofolate	Trimethoprim	95.8 ± 2.2	<0.1	<0.1
Beta-blockers	Propranolol	104.5 ± 4.1	<0.1	0.1
	Atenolol	97.7 ± 3.0	<0.1	<0.1
Psychiatric drugs and stimulants	Carbamazepine	28.6 ± 0.1	<0.1	<0.1
	Caffeine	353359.8 ± 14343	0.1	0.3
To treat Asthma	Albuterol	11.8 ± 1.2	<0.1	0.1

[1] LOD = Limit of Detection

[2] LOQ = Limit of Quantification

Concentrations of 10 PhACs (ibuprofen, diclofenac, clarithromycin, ofloxacin, norfloxacin, propranolol, atenolol, carbamazepine, and caffeine) detected in the studied effluent were higher than the mean concentrations of these PhACs in wastewater effluents in European Union. Only four of the analyzed PhACs (acetaminophen, gemfibrozil, sulfadiazine, and sulfamethoxazole) were below mean concentration and the rest of the studied PhACs were not included in the list of the most commonly detected chemicals in European Union WWTP effluents [51].

Photocatalytic decomposition of PhACs detected in wastewater effluent was conducted using 1 g L^{-1} of 4%-Gd-$BiVO_4$ according to experimental findings and literature review stated in section 3.2.1. The concentration of the 22 studied PhACs was measured before photocatalytic tests, after establishing adsorption equilibrium (30 min in the absence of UVA), and after 180 min of photocatalytic test (UVA dose = 139.5 Wh m^{-2}, t_{30W} = 279 min^{-1}). Moreover, a reference adsorption test was carried out in order to confirm the photocatalytic nature of pharmaceuticals decomposition. It should be stressed that some of the PhACs detected in wastewater effluent can be easily photodegraded under UVA irradiation (photolysis) [52]. Therefore, a reference photolysis test was conducted, and the decomposition of PhACs was measured. The results are shown in Figure 7.

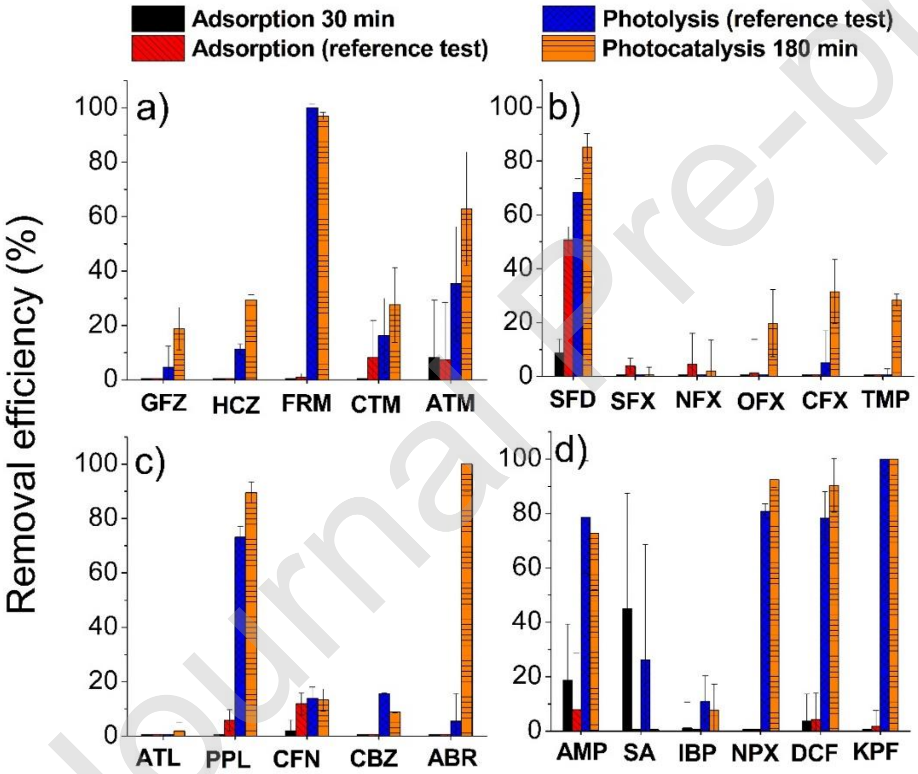

Figure 7. Removal of PhACs from urban wastewater effluent by photocatalysis (1 g L^{-1} of 4%-Gd-$BiVO_4$; UVA dose = 139.5 Wh m^{-2}, t_{30W} = 279 min^{-1}), photolysis (180 min; UVA dose = 139.5 Wh m^{-2}, t_{30W} = 279 min^{-1}), and adsorption (1 g L^{-1} of 4%-Gd-$BiVO_4$ in absence of light). **a)** Lipid regulators, diuretics and macrolides: Gemfibrozil (GFZ), Hydrochlorothiazide (HCZ), Furosemide (FRM), Clarithromycin (CTM), and Azithromycin (ATM). **b)** Sulfonamides, quinolones and dihydrofolate: Sulfadiazine (SFD), Sulfamethoxazole (SFX), Norfloxacin (NFX), Ofloxacin (OFX), Ciprofloxacin (CFX), and Trimethoprim (TMP). **c)** Beta-blockers, psychiatric drugs and stimulants to treat asthma: Atenolol (ATL), Propranolol (PPL), Caffeine

(CFN), Carbamazepine (CBZ), and Albuterol (ABR). **d)** Anti-inflammatories: Acetaminophen (AMP), Salicylic Acid (SA), Ibuprofen (IBP), Naproxen (NPX), Diclofenac (DCF), and Ketoprofen (KPF).

The removal efficiencies of the studied PhACs varied from negative to 100% removal depending on the compound. The apparent negative removal efficiencies probably resulted from the transformation of the conjugated forms into the original parent compounds during treatment [1]. For the purpose of this study, all the negative efficiencies were considered as zero. As observed in Figure 7a poor photocatalytic removal efficiency was observed for lipid regulator gemfibrozil (18.9%), while negligible and null elimination was observed after photolysis and adsorption tests. Removal of diuretics did not follow a similar pathway. Hence, high removal efficiency of furosemide was observed after photocatalysis (97%) and photolysis (100%), while hydrochlorothiazide showed poor removal after photocatalytic treatment (29.4%) and photolytic treatment (11.3%). Adsorption leads to negligible or null elimination of diuretics from wastewater effluent.

Macrolides detected in wastewater effluent, namely azithromycin and clarithromycin are compounds included to the second the Watch List (Directive 2018/840/EU). Under applied experimental conditions (180 min of contact time; UVA dose = 139.5 Wh m^{-2}, t_{30W} = 279 min^{-1}), poor and moderate photocatalytic removal efficiencies were achieved for clarithromycin (27.5%) and azithromycin (62.9%). It should be mentioned that the removal efficiency of the two macrolides was about twice higher when photocatalysis was used as compared to photolysis.

Sulfonamides detected in wastewater effluent behaved in different ways during photocatalytic treatment (Figure 7b). High photocatalytic removal efficiency was observed for sulfadiazine (85.1%) while sulfamethoxazole showed 0% removal. Similarly, after photolysis moderate removal was achieved for sulfadiazine (68.5%) and 0% for sulfamethoxazole. Poor removal efficiencies were observed during photocatalysis for all detected quinolones, among which ciprofloxacin is a compound included in the second Watch List (Directive 2018/840/EU). Photolysis and adsorption led to negligible elimination of quinolones. Interestingly, complete photolytic elimination of ciprofloxacin was reported in earlier studies [52], while in this study about 5% of removal was observed. However, these results can be attributed to differences in irradiation sources and received UV doses. Trimethoprim also showed poor photocatalytic decomposition (28.3%) and negligible or null elimination after photolysis and adsorption.

As it is shown in Figure 7c, a difference in the behavior of detected beta-blockers was observed during photocatalytic tests. For instance, high photocatalytic removal efficacy was achieved for propranolol (89.5%), while this value was negligible for atenolol (2%). 0% removal was achieved after photolysis for atenolol and high removal was observed for propranolol

(73.1%), which is in agreement with results reported by Baena-Nogueras et al., (2017). For such compounds as caffeine and carbamazepine poor removal efficiencies were achieved after photocatalytic treatment, while similar or slightly higher elimination was observed after photolysis. These results are in agreement with an earlier study [52], in which carbamazepine (initial concentration 100 ng L^{-1}) was not eliminated by photolysis. Complete removal of albuterol (asthma treatment) was observed after the photocatalytic test (180 min of contact time; UVA dose = 139.5 Wh m^{-2}, t_{30W} = 279 min^{-1}), while photolysis and adsorption led to negligible and null elimination of this compound. These results are in agreement with a study by Baena-Nogueras et al., (2017), in which photolysis did not lead to the removal of albuterol from water.

As can be seen from the Figure 7d anti-inflammatories were removed with high (80 – 100 %; naproxen, diclofenac and ketoprofen), moderate (40 – 70 %; acetaminophen), poor (< 30 %; ibuprofen) and null (0%; salicylic acid) efficiency by photocatalysis (180 min of contact time; UVA dose = 139.5 Wh m^{-2}, t_{30W} = 279 min^{-1}). It is important to mention that moderate and high removal efficiencies were achieved by UVA-LED photolysis for acetaminophen, naproxen, diclofenac, and ketoprofen. The obtained results are in agreement with an earlier study, in which very high (99%) removal of diclofenac (initial concentration of 100 ng L^{-1}) was reported by photolysis under simulated solar irradiation [52]. A moderate removal efficiency was obtained for acetaminophen by photocatalysis (72.7%) and UVA-LED photolysis (78.7%). For the elimination of naproxen, photolysis was slightly less efficient (81%) in comparison with photocatalysis, while ketoprofen achieved complete elimination by both photolytic and photocatalytic processes. Also, another study reported almost complete elimination of naproxen (initial concentration similar to that in our study) and diclofenac (initial concentration about twice as high as in our study) during solar photocatalysis with TiO_2 at t_{30W} below 150 and 300 min, respectively [6]. The elimination of ibuprofen and salicylic acid during photolysis was poor. It should be noted that adsorption of studied anti-inflammatories onto photocatalyst was poor or negative except for salicylic acid. Moderate adsorption removal of salicylic acid (45%) was achieved after 30 min of contact time, while 0% removal was observed after the adsorption reference test (210 min of contact time), which suggests possible desorption of salicylic acid from the photocatalysts.

It should be mentioned that TOC and COD values were monitored during photocatalysis with 4%-Gd-$BiVO_4$ (1 g L^{-1}) and photolysis (results are not shown for the sake of brevity). However, no reduction of TOC or COD was detected during 3 h of photocatalysis and photolysis, indicating relatively low photocatalytic activity. The obtained results are in agreement with an earlier study [31], where no reduction of TOC in secondary effluent was reported after 5h of solar photocatalysis with Ag/$BiVO_4$ (dose 0.5 and 1 g L^{-1}). Moreover, the concentration of dissolved metals and rare earth (Bi, V, and Gd) was measured before and after photocatalytic treatment by means of ICP-OES to evaluate the physicochemical stability of 4%-Gd-BiVO$_4$ and to ensure that the photocatalyst does not release toxic metals to the effluent during photocatalysis. None of the three analysed elements were detected in the effluent either before or after the photocatalytic treatment. Hence, it can be assumed that 4%-Gd-BiVO$_4$ photocatalyst has good stability.

3.3 Photocatalytic efficiency of 4%-Gd-BiVO$_4$ for bacterial inactivation.

Photocatalytic efficiency was also addressed for bacterial inactivation. As discussed in section 3.2.1, photocatalytic inactivation of bacteria detected in wastewater effluent was conducted using 1 g L^{-1} of 4%-Gd-BiVO$_4$, which agrees with available literature [31]. Selected examples of inactivation profiles belonging to *Enterococci* and *K. pneumoniae* species are depicted in Figure 8 a-b where the different processes, namely photolysis, 4%-Gd-BiVO$_4$ photocatalysis, and adsorption showed different inactivation routes. Firstly, adsorption onto the photocatalyst (in absence of UVA-LED light) reached slight inactivation on the different bacteria, i.e. 0.11, 0.15, 0.19, and 0.91 Log-removal values (LRV) were obtained for *T. coliforms*, *K. pneumoniae*, *E. coli,* and *Enterococci*, respectively. In the case of photolysis and 4%-Gd-BiVO$_4$-photocatalysis, notably major rates of inactivation were obtained. Kinetic rate constants for these two processes are represented in Figure 8 c.

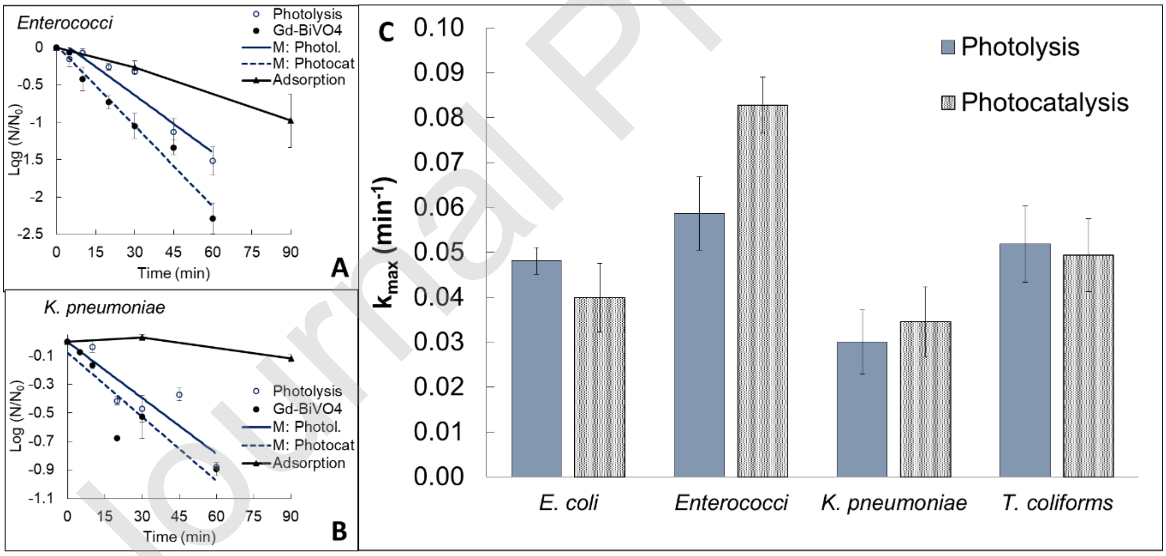

Figure 8. Selected examples of inactivation profiles obtained for **a)** *Enterococci,* and **b)** *K. pneumoniae.* Log-lineal model (M) is represented with lines on Photolysis and Photocatalytic processes (a,b). **C)** Kinetic rate constants (min^{-1}) obtained for photolytic (UVA-LED) and photocatalytic (1 g L^{-1} of 4%-Gd-BiVO$_4$ + UVA-LED) inactivation of *E. coli*, *Enterococci*, *K. pneumoniae*, and T. coliforms.

Photolysis showed effectivity itself for bacterial inactivation. *K. pneumoniae* was the most resistant bacteria, since the LRV was not reached at 60 min of exposure time, with a k$_{max}$ of

0.03 ± 0.10 min^{-1} in comparison with the k_{max} obtained for the rest of bacteria which is in the range of 0.05-0.06 min^{-1}. It is known that direct UVA can inflict not only direct and indirect DNA damage, but also oxidative damages since some cell components absorb in the UVA region, such as catalase [53]. Thus, the higher resistance of *K. pneumoniae* can be attributed to their cellular structure. Particularly, it has been reported that *K. pneumoniae* have robust capsules that can protect it from bactericidal stressors, such as UV irradiation [54,55].

In comparison with single photolysis, an improvement in bacteria inactivation during photocatalytic processes was obtained for *Enterococci* which was quantified in an increase on k_{max} by 41.1%, which means that the time for reach 1 LRV was reduced from 44.4 min (UVA) to 28.8 min (UVA/4%-Gd-$BiVO_4$). Nevertheless, this photocatalytic enhancement has not been detected for *E. coli* and T. coliforms. Also, *K. pneumoniae* showed a similar behaviour during photolysis and photocatalysis. The trend observed for bacterial inactivation by photocatalysis was *Enterococci* > *T. coliforms* > *E. coli* > *K. pneumoniae*. It is important to note that UV-transmittance at 370 nm notably differs in the absence of the photocatalyst (79.2%) and in the presence of it (25.7%). This has important implications in the experimental set-up since the mean UVA intensity within the photo-reactor markedly decreases. Accordingly, results reported of photocatalytic processes were obtained with rather low photonic flux in comparison with UVA photolysis, so it can be assumed that in every case, higher efficiencies are expected in the presence of photocatalyst.

As previously commented, the cell structure of the different bacteria can have a direct relationship with caused oxidative damages. For instance, *E. coli,* as gram negative bacteria are known to be sensitive to UV light, especially at high intensities [39]. This high sensitivity to UVA radiation might lead to more effective bacteria inactivation in photolysis as compared to photocatalytic processes [39,56,57] as was also observed in this study (Figure 8c). On the other hand, it was observed that *Enterococci,* which is a gram positive bacteria, showed higher sensitivity to the photocatalytic process than to the photolytic one. Lastly, as observed in Figure 9 c, *K. pneumoniae* showed very similar inactivation rates in the presence of 4%-Gd-$BiVO_4$ (photocatalysis) and under direct UVA-LED radiation (photolysis). However, it is still is the most resistant bacteria against oxidative damages, suggesting the prominent capsule of these cells could protect it from direct attacks from oxidant radicals [54,55]. Though, if longer reaction times are applied, a complete inactivation can be possibly reached.

Another factor that should be taken into account is the interaction between photocatalysts and bacteria [39,42,58]. Close contact is required between bacteria and photocatalyst, since the adhesion onto the photocatalyst surface is positively correlated to the inactivation efficiency. This can be explained considering that photo-generated radicals are most likely present at photocatalyst surface and because of its short lifetime may easily interact with adsorbed bacteria, damaging its cell wall and consequently favoring bacteria inactivation [39]. In this regard, dark tests revealed that *Enterococci* showed higher adhesion onto the photocatalyst (0.91 LRV) what explains the higher photocatalytic inactivation of this group as compared to the other bacterial models studied.

Previous disinfection studies using $BiVO_4$ as photocatalyst have been reported [27,31,42,59]. For instance, Sharma et al. (2016), Adán et al. (2015), and Adán et al. (2016) reported high photocatalytic activity and higher antimicrobial activity in deionized water towards *E. coli* when it is compared with simple photolysis. Booshehri et al. (2017) reported similar results, in which the photocatalytic effect was also effective in well water and secondary wastewater effluent. However, they assessed the inactivation efficacy with pure strains spiked to the water matrices. These changes in experimental set-up (e.g. initial concentration of microorganisms or radiation intensities) make inactivation ratios difficult to compare between the different studies. Nonetheless, our results agree with these trends since the efficacy of 4%-Gd-$BiVO_4$ photocatalyst has also been confirmed in this study.

4. Conclusions

Photocatalytic activity of Gd^{3+} doped $BiVO_4$ was investigated through the decomposition of diclofenac in ultra-pure water (model solution) and 22 different PhACs from real urban wastewater effluent. In addition, photocatalytic inactivation of Total coliforms, *Escherichia coli, Enterococci*, and *Klebsiella pneumoniae* present in wastewater effluent was assessed. A UVA-LED lamp was used as irradiation source in all the performed photocatalytic studies. Concluding remarks can be summarized as follows:

- Characterization results of X-ray diffraction and X-ray photoelectron spectroscopy demonstrated that the crystalline structure of $BiVO_4$ was successfully doped by the Gd^{3+} ions. Moreover, three crystalline structures were identified forming a heterostructure that may favor the separation of charge carriers.
- The effect of 4%-Gd-$BiVO_4$ concentration on the initial disappearance rate of the diclofenac model solution was evaluated and a concentration of 1 g L^{-1} was found to be the optimal photocatalyst dose. At the optimal dose, diclofenac decomposition reached up to 98.3% after 120 min under UVA-LED light.
- No dissolved metals (Bi, V, or Gd) were detected in effluent either before or after photocatalytic experiments. This suggests that 4%-Gd-$BiVO_4$ has good stability and that there will be no leaching of toxic metals in the treated effluent.
- The photocatalytic removal of PhACs in wastewater was quite variable due to the complexity of the matrix and physicochemical characteristics of each studied

contaminant. Thus, high photocatalytic removal efficiency (80 – 100%) was observed for some of the studied PhACs such as naproxen, diclofenac, ketoprofen, and furosemide. On the other hand, other PhACs showed moderate removal efficiency (40 – 70%) for example, acetaminophen and azithromycin. Some of the studied PhACs such as clarithromycin or Ibuprofen showed poor removal efficiency (<30%).

- Although the irradiation (UVA-LED) by itself caused inactivation in all microbes tested, the bigger improvement from the photocatalytic treatment was appreciable in *Enterococci* bacterial indicator by increasing the k_{max} in 41.1%. *Enterococci* were the most sensitive bacteria to photocatalytic treatment whereas *K. pneumoniae* showed the highest resistance for both processes.
- The capability of 4%-Gd-$BiVO_4$ for bacteria inactivation and PhACs elimination from real wastewater effluent was demonstrated at laboratory scale. However, not significant changes were observed on TOC and COD values of wastewater effluent after photocatalytic treatment (180 min of contact time; UVA dose = 139.5 Wh m^{-2}, t_{30W} = 279 min^{-1}). Thus, further studies are required in order to improve the photocatalytic activity of the synthesized material for possible up-scale application in wastewater treatment.

CRediT author statement

C. Orona-Návar: Conceptualization, Methodology, Investigation, Validation, Visualization, Writing – Original Draft; **I. Levchuk:** Conceptualization, Methodology, Investigation, Validation, Writing – Original Draft; **J. Moreno-Andrés:** Conceptualization, Methodology, Investigation, Validation, Writing – Original Draft; **Y. Park:** Supervision, Writing – Review & editing; **J. Mahlknecht:** Supervision, Writing – Review & editing; **A. Mikola:** Resources, Supervision, Writing – Review & editing; **M. Sillanpää:** Resources, Supervision, Writing – Review & editing **N. Ornelas-Soto:** Resources, Supervision, Project administration, Writing – Review & editing, Funding acquisition.

Declaration of interests

The authors declare that they have no known competing financial interests or personal relationships that could have appeared to influence the work reported in this paper.

Acknowledgments

Authors are grateful for funding received from KAUTE säätiö (grant number: 201800116) and Consejo Nacional de Ciencia y Tecnología (CONACyT) through scholarship #583166 and #291250. Dr. J. Moreno-Andrés acknowledges the financial support by the 2014-2020 ERDF Operational Programme and by the Department of Economy, Knowledge, Business and University of the Regional Government of Andalusia. Project reference: FEDER-UCA18-108023".

References

[1] N.H. Tran, M. Reinhard, K.Y.-H. Gin, Occurrence and fate of emerging contaminants in municipal wastewater treatment plants from different geographical regions-a review, Water Res. 133 (2018) 182–207. doi:10.1016/J.WATRES.2017.12.029.

[2] T. Deblonde, C. Cossu-Leguille, P. Hartemann, Emerging pollutants in wastewater: A review of the literature, Int. J. Hyg. Environ. Health. 214 (2011) 442–448. doi:10.1016/j.ijheh.2011.08.002.

[3] I.Y. López-Pacheco, A. Silva-Núñez, C. Salinas-Salazar, A. Arévalo-Gallegos, L.A. Lizarazo-Holguin, D. Barceló, H.M.N. Iqbal, R. Parra-Saldívar, Anthropogenic contaminants of high concern: Existence in water resources and their adverse effects, Sci. Total Environ. 690 (2019) 1068–1088. doi:10.1016/j.scitotenv.2019.07.052.

[4] A. Chiffre, F. Degiorgi, A. Bulete, L. Spinner, P.M. Badot, Occurrence of pharmaceuticals in WWTP effluents and their impact in a karstic rural catchment of Eastern France, Environ. Sci. Pollut. Res. 23 (2016) 25427–25441. doi:10.1007/s11356-016-7751-5.

[5] European Comision, COMMISSION IMPLEMENTING DECISION (EU) 2018/ 840 establishing a watch list of substances for Union-wide monitoring in the field of water policy pursuant to Directive 2008/105/EC of the European Parliament and of the Council and repealing Commission Impleme, Brussels, 2018.

[6] L. Prieto-Rodriguez, S. Miralles-Cuevas, I. Oller, a Agüera, G. Li Puma, S. Malato, Treatment of emerging contaminants in wastewater treatment plants (WWTP) effluents by solar photocatalysis using low TiO2 concentrations., J. Hazard. Mater. 211–212 (2012) 131–7. doi:10.1016/j.jhazmat.2011.09.008.

[7] L. Rizzo, S. Malato, D. Antakyali, V.G. Beretsou, M.B. Đolić, W. Gernjak, E. Heath, I. Ivancev-Tumbas, P. Karaolia, A.R. Lado Ribeiro, G. Mascolo, C.S. McArdell, H. Schaar, A.M.T. Silva, D. Fatta-Kassinos, Consolidated vs new advanced treatment methods for the removal of contaminants of emerging concern from urban wastewater, Sci. Total Environ. 655 (2019) 986–1008. doi:10.1016/j.scitotenv.2018.11.265.

[8] G. Maniakova, K. Kowalska, S. Murgolo, G. Mascolo, G. Libralato, G. Lofrano, O. Sacco, M. Guida, L. Rizzo, Comparison between heterogeneous and homogeneous solar driven advanced oxidation processes for urban wastewater treatment: Pharmaceuticals removal and toxicity, Sep. Purif. Technol. 236 (2020). doi:10.1016/j.seppur.2019.116249.

[9] J. You, Y. Guo, R. Guo, X. Liu, A review of visible light-active photocatalysts for water disinfection: Features and prospects, Chem. Eng. J. 373 (2019) 624–641. doi:10.1016/j.cej.2019.05.071.

[10] G. Iervolino, I. Zammit, V. Vaiano, L. Rizzo, Limitations and Prospects for Wastewater Treatment by UV and Visible-Light-Active Heterogeneous Photocatalysis: A Critical Review, Top. Curr. Chem. 378 (2020) 1–40. doi:10.1007/s41061-019-0272-1.

[11] P. Ganguly, C. Byrne, A. Breen, S.C. Pillai, Antimicrobial activity of photocatalysts: Fundamentals, mechanisms, kinetics and recent advances, Appl. Catal. B Environ. 225 (2018) 51–75. doi:10.1016/j.apcatb.2017.11.018.

[12] B. Tryba, S. Jafari, M. Sillanpää, A. Nitta, B. Ohtani, A.W. Morawski, Influence of TiO2 structure on its photocatalytic activity towards acetaldehyde decomposition, Appl. Surf. Sci. 470 (2019) 376–385. doi:10.1016/j.apsusc.2018.11.137.

[13] L. V. Bora, R.K. Mewada, Visible/solar light active photocatalysts for organic effluent

treatment: Fundamentals, mechanisms and parametric review, Renew. Sustain. Energy Rev. 76 (2017) 1393–1421. doi:10.1016/j.rser.2017.01.130.

[14] S. Helali, M.I. Polo-López, P. Fernández-Ibáñez, B. Ohtani, F. Amano, S. Malato, C. Guillard, Solar photocatalysis: A green technology for E. coli contaminated water disinfection. Effect of concentration and different types of suspended catalyst, J. Photochem. Photobiol. A Chem. 276 (2014) 31–40. doi:10.1016/j.jphotochem.2013.11.011.

[15] A. Malathi, J. Madhavan, M. Ashokkumar, P. Arunachalam, A review on BiVO4 photocatalyst: Activity enhancement methods for solar photocatalytic applications, Appl. Catal. A Gen. 555 (2018) 47–74. doi:10.1016/j.apcata.2018.02.010.

[16] W. Jo, R.J. Tayade, New Generation Energy-Efficient Light Source for Photocatalysis : LEDs for Environmental Applications, Ind. Eng. Chemestry Res. 53 (2014) 2073–2084.

[17] I. Levchuk, M. Kralova, J.J. Rueda-Márquez, J. Moreno-Andrés, S. Gutiérrez-Alfaro, P. Dzik, S. Parola, M. Sillanpää, R. Vahala, M.A. Manzano, Antimicrobial activity of printed composite TiO2/SiO2 and TiO2/SiO2/Au thin films under UVA-LED and natural solar radiation, Appl. Catal. B Environ. 239 (2018) 609–618. doi:10.1016/J.APCATB.2018.08.051.

[18] L.H. Levine, J.T. Richards, J.L. Coutts, R. Soler, F. Maxik, R.M. Wheeler, Feasibility of ultraviolet-light-emitting diodes as an alternative light source for photocatalysis, J. Air Waste Manag. Assoc. 61 (2011) 932–940. doi:10.1080/10473289.2011.596746.

[19] S.D. Dolić, D.J. Jovanović, K. Smits, B. Babić, M. Marinović-Cincović, S. Porobić, M.D. Dramićanin, A comparative study of photocatalytically active nanocrystalline tetragonal zyrcon-type and monoclinic scheelite-type bismuth vanadate, Ceram. Int. 44 (2018) 17953–17961. doi:10.1016/j.ceramint.2018.06.272.

[20] X. Chen, L. Li, T. Yi, W. Zhang, X. Zhang, L. Wang, Microwave assisted synthesis of sheet-like Cu/BiVO<inf>4</inf> and its activities of various photocatalytic conditions, J. Solid State Chem. 229 (2015) 141–149. doi:10.1016/j.jssc.2015.05.026.

[21] E.M. Siedlecka, Application of Bismuth-Based Photocatalysts in Environmental Protection, in: Inamuddin, A. Asiri, E. Lichtfouse (Eds.), Nanophotocatalysis Environ. Appl. Environ. Chem. a Sustain. World, Springer Cham, Switzerland, 2020: pp. 87–118. doi:10.1007/978-3-030-12619-3_4.

[22] X. Meng, Z. Zhang, Bismuth-based photocatalytic semiconductors: Introduction, challenges and possible approaches, J. Mol. Catal. A Chem. 423 (2016) 533–549. doi:10.1016/j.molcata.2016.07.030.

[23] R. He, S. Cao, P. Zhou, J. Yu, Recent advances in visible light Bi-based photocatalysts, Chinese J. Catal. 35 (2014) 989–1007. doi:10.1016/s1872-2067(14)60075-9.

[24] S. Obregón, G. Colón, On the origin of the photocatalytic activity improvement of BIVO4 through rare earth tridoping, Appl. Catal. A Gen. 501 (2015) 56–62. doi:10.1016/j.apcata.2015.04.032.

[25] X. Luo, G. Zhu, J. Peng, X. Wei, M. Hojamberdiev, L. Jin, P. Liu, Enhanced photocatalytic activity of Gd-doped porous β-Bi2O3 photocatalysts under visible light irradiation, Appl. Surf. Sci. 351 (2015) 260–269. doi:10.1016/j.apsusc.2015.05.137.

[26] X. Gao, Z. Wang, X. Zhai, F. Fu, W. Li, The synthesize of lanthanide doped BiVO4 and its enhanced photocatalytic activity, J. Mol. Liq. 211 (2015) 25–30. doi:10.1016/J.MOLLIQ.2015.06.058.

[27] C. Adán, J. Marugán, S. Obregón, G. Colón, Photocatalytic Escherichia coli inactivation

by means of trivalent Er3+, Y3+ doping of BiVO4 system, Appl. Catal. A Gen. 526 (2016) 126–131. doi:10.1016/j.apcata.2016.08.002.

[28] A.M. Al-Hamdi, M. Sillanpää, J. Dutta, Gadolinium doped tin dioxide nanoparticles: an efficient visible light active photocatalyst, J. Rare Earths. 33 (2015) 1275–1283. doi:10.1016/S1002-0721(14)60557-3.

[29] A.W. Xu, Y. Gao, H.Q. Liu, The preparation, characterization, and their photocatalytic activities of rare-earth-doped TiO2 nanoparticles, J. Catal. 207 (2002) 151–157. doi:10.1006/jcat.2002.3539.

[30] A.P. Reverberi, P.S. Varbanov, M. Vocciante, B. Fabiano, Bismuth oxide-related photocatalysts in green nanotechnology: A critical analysis, Front. Chem. Sci. Eng. 12 (2018) 878–892. doi:10.1007/s11705-018-1744-5.

[31] A.Y. Booshehri, M.I. Polo-Lopez, M. Castro-Alférez, P. He, R. Xu, W. Rong, S. Malato, P. Fernández-Ibáñez, Assessment of solar photocatalysis using Ag/BiVO4 at pilot solar Compound Parabolic Collector for inactivation of pathogens in well water and secondary effluents, Catal. Today. 281 (2017) 124–134. doi:10.1016/J.CATTOD.2016.08.016.

[32] A.R. Lado Ribeiro, N.F.F. Moreira, G. Li Puma, A.M.T. Silva, Impact of water matrix on the removal of micropollutants by advanced oxidation technologies, Chem. Eng. J. 363 (2019) 155–173. doi:10.1016/j.cej.2019.01.080.

[33] R.S. Ribeiro, Z. Frontistis, D. Mantzavinos, A.M. T Silva, J.L. Faria, H.T. Gomes, Screening of heterogeneous catalysts for the activated persulfate oxidation of sulfamethoxazole in aqueous matrices. Does the matrix affect the selection of catalyst?, J. Chem. Technol. Biotechnol. 94 (2019) 2425–2432. doi:10.1002/jctb.6080.

[34] R. María Baena-Nogueras, M. G. Pintado-Herrera, E. González-Mazo, P. A. Lara-Martín, Determination of Pharmaceuticals in Coastal Systems Using Solid Phase Extraction (SPE) Followed by Ultra Performance Liquid Chromatography – tandem Mass Spectrometry (UPLC-MS/MS), Curr. Anal. Chem. 12 (2016) 183–201. doi:10.2174/1573411012666151009193254.

[35] W. Yin, W. Wang, M. Shang, L. Zhou, S. Sun, L. Wang, BiVO4 Hollow Nanospheres: Anchoring Synthesis, Growth Mechanism, and Their Application in Photocatalysis, Eur. J. Inorg. Chem. (2009) 4379–4384. doi:10.1002/ejic.200900614.

[36] M. Sevilla, A.B. Fuertes, Chemical and Structural Properties of Carbonaceous Products Obtained by Hydrothermal Carbonization of Saccharides, Chem. - A Eur. J. 15 (2009) 4195–4203. doi:10.1002/chem.200802097.

[37] D. Stülten, S. Zühlke, M. Lamshöft, M. Spiteller, Occurrence of diclofenac and selected metabolites in sewage effluents, Sci. Total Environ. 405 (2008) 310–316. doi:10.1016/j.scitotenv.2008.05.036.

[38] American Public Health Association, Standard Methods for the Examination of Water & Wastewater, 2005.

[39] I. Levchuk, T. Homola, J. Moreno-Andrés, J.J. Rueda-Márquez, P. Dzik, M.Á. Moríñigo, M. Sillanpää, M.A. Manzano, R. Vahala, Solar photocatalytic disinfection using ink-jet printed composite TiO2/SiO2 thin films on flexible substrate: Applicability to drinking and marine water, Sol. Energy. 191 (2019) 518–529. doi:10.1016/j.solener.2019.09.038.

[40] K. Zhong, H. Gao, J. Feng, Y. Zhang, K. Lai, Facile synthesis of Z-scheme Se/BiVO 4 heterojunction with enhanced visible-light-driven photocatalytic performance, J. Mater.

Sci. 54 (2019) 10632–10643. doi:10.1007/s10853-019-03634-1.

[41] Q. Yuan, L. Chen, M. Xiong, J. He, S.L. Luo, C.T. Au, S.F. Yin, Cu2O/BiVO4 heterostructures: Synthesis and application in simultaneous photocatalytic oxidation of organic dyes and reduction of Cr(VI) under visible light, Chem. Eng. J. 255 (2014) 394–402. doi:10.1016/j.cej.2014.06.031.

[42] C. Adán, J. Marugán, S. Obregón, G. Colón, Photocatalytic activity of bismuth vanadates under UV-A and visible light irradiation: Inactivation of Escherichia coli vs oxidation of methanol, Catal. Today. 240 (2015) 93–99. doi:10.1016/j.cattod.2014.03.059.

[43] O. Monfort, G. Plesch, Bismuth vanadate-based semiconductor photocatalysts : a short critical review on the efficiency and the mechanism of photodegradation of organic pollutants, Environ. Sci. Pollut. Res. 25 (2018) 19362–19379.

[44] C. Regmi, Y.K. Kshetri, R.P. Pandey, S.W. Lee, Visible-light-driven S and W co-doped dendritic BiVO4 for efficient photocatalytic degradation of naproxen and its mechanistic analysis, Mol. Catal. 453 (2018) 149–160. doi:10.1016/j.mcat.2018.05.008.

[45] M. Wang, H. Zheng, Q. Liu, C. Niu, Y. Che, M. Dang, High performance B doped BiVO4 photocatalyst with visible light response by citric acid complex method, Spectrochim. Acta Part A Mol. Biomol. Spectrosc. 114 (2013) 74–79. doi:10.1016/J.SAA.2013.05.032.

[46] M. Moradi, G. Moussavi, K. Yaghmaeian, A. Yazdanbakhsh, V. Srivastava, M. Sillanpää, Synthesis of novel Ag-doped S-MgO nanosphere as an efficient UVA/LED-activated photocatalyst for non-radical oxidation of diclofenac: Catalyst preparation and characterization and photocatalytic mechanistic evaluation, Appl. Catal. B Environ. 260 (2020) 118128. doi:10.1016/j.apcatb.2019.118128.

[47] I. Tbessi, M. Benito, J. Llorca, E. Molins, S. Sayadi, W. Najjar, Silver and manganese co-doped titanium oxide aerogel for effective diclofenac degradation under UV-A light irradiation, J. Alloys Compd. 779 (2019) 314–325. doi:10.1016/j.jallcom.2018.11.083.

[48] V.C. Sarasidis, K. V. Plakas, S.I. Patsios, A.J. Karabelas, Investigation of diclofenac degradation in a continuous photo-catalytic membrane reactor. Influence of operating parameters, Chem. Eng. J. 239 (2014) 299–311. doi:10.1016/j.cej.2013.11.026.

[49] A.S. Mestre, A.P. Carvalho, Photocatalytic degradation of pharmaceuticals carbamazepine, diclofenac, and sulfamethoxazole by semiconductor and carbon materials: A review, Molecules. 24 (2019). doi:10.3390/molecules24203702.

[50] J.J. Rueda-Marquez, I. Levchuk, P. Fernández Ibañez, M. Sillanpää, A critical review on application of photocatalysis for toxicity reduction of real wastewaters, J. Clean. Prod. (2020) 120694. doi:10.1016/j.jclepro.2020.120694.

[51] R. Loos, R. Carvalho, D.C. António, S. Comero, G. Locoro, S. Tavazzi, B. Paracchini, M. Ghiani, T. Lettieri, L. Blaha, B. Jarosova, S. Voorspoels, K. Servaes, P. Haglund, J. Fick, R.H. Lindberg, D. Schwesig, B.M. Gawlik, EU-wide monitoring survey on emerging polar organic contaminants in wastewater treatment plant effluents, Water Res. 47 (2013) 6475–6487. doi:10.1016/j.watres.2013.08.024.

[52] R.M. Baena-Nogueras, E. González-Mazo, P.A. Lara-Martín, Degradation kinetics of pharmaceuticals and personal care products in surface waters: photolysis vs biodegradation, Sci. Total Environ. 590–591 (2017) 643–654. doi:10.1016/j.scitotenv.2017.03.015.

[53] S. Giannakis, M.I. Polo López, D. Spuhler, J.A. Sánchez Pérez, P. Fernández Ibáñez,

C. Pulgarin, Solar disinfection is an augmentable, in situ-generated photo-Fenton reaction—Part 1: A review of the mechanisms and the fundamental aspects of the process, Appl. Catal. B Environ. 199 (2016) 199–223. doi:10.1016/j.apcatb.2016.06.009.

[54] S. Aguilar, D. Rosado, J. Moreno-Andrés, L. Cartuche, D. Cruz, A. Acevedo-Merino, E. Nebot, Inactivation of a wild isolated Klebsiella pneumoniae by photo-chemical processes: UV-C, UV-C/H2O2 and UV-C/H2O2/Fe3+, Catal. Today. 313 (2018) 94–99. doi:10.1016/j.cattod.2017.10.043.

[55] D. Venieri, I. Gounaki, M. Bikouvaraki, V. Binas, A. Zachopoulos, G. Kiriakidis, D. Mantzavinos, Solar photocatalysis as disinfection technique: Inactivation of Klebsiella pneumoniae in sewage and investigation of changes in antibiotic resistance profile, J. Environ. Manage. 195 (2017) 140–147. doi:10.1016/j.jenvman.2016.06.009.

[56] A.K. Benabbou, Z. Derriche, C. Felix, P. Lejeune, C. Guillard, Photocatalytic inactivation of Escherischia coli. Effect of concentration of TiO2 and microorganism, nature, and intensity of UV irradiation, Appl. Catal. B Environ. 76 (2007) 257–263. doi:10.1016/j.apcatb.2007.05.026.

[57] J. Rodríguez-Chueca, S. Guerra-Rodríguez, J.M. Raez, M.J. López-Muñoz, E. Rodríguez, Assessment of different iron species as activators of S2O82- and HSO5- for inactivation of wild bacteria strains, Appl. Catal. B Environ. 248 (2019) 54–61. doi:10.1016/j.apcatb.2019.02.003.

[58] C. Pablos, R. Van Grieken, J. Marugán, I. Chowdhury, S.L. Walker, Study of bacterial adhesion onto immobilized TiO2: Effect on the photocatalytic activity for disinfection applications, Catal. Today. 209 (2013) 140–146. doi:10.1016/j.cattod.2012.12.010.

[59] R. Sharma, Uma, S. Singh, A. Verma, M. Khanuja, Visible light induced bactericidal and photocatalytic activity of hydrothermally synthesized BiVO 4 nano-octahedrals, J. Photochem. Photobiol. B Biol. 162 (2016) 266–272. doi:10.1016/j.jphotobiol.2016.06.035.